A MODEL FOR MARTIAN MAGMA OCEAN CRYSTALLIZATION AND OVERTURN. L. T. Elkins-Tanton, E. M. Parmentier, and P.C. Hess, Brown University (Department of Geological Sciences, Providence RI 02912; Linda_Elkins_Tanton@brown.edu, EM_Parmentier@brown.edu).

Introduction: Early Mars is assumed to have melted completely during accretion. Solidification of this magma ocean determines initial planetary compositional differentiation and the stability of the mantle density profile, which in turn have significance for magmatic source regions, convective instability, and magnetic field generation. Excellent progress on the dynamical problem of magma ocean crystallization has been made (*c.f.*, [1, 2]), but the dynamic and compositional results of crystallizing a magma ocean have not previously been investigated specifically for Mars.

The goals of this study are to create a simple model for Martian magma ocean crystallization and assess the outcome of overturn due to density instability. We explore the possibility that this can explain aspects of the Martian magnetic field and can reproduce the compositions of Martian meteorite source regions.

Methods and Models: The bulk composition of the Martian mantle is assumed to be that of Bertka and Fei [3] renormalized without Na_2O. The mantle is assumed to be 2000 km deep, with a pressure of 24 GPa at the core-mantle boundary. As the magma ocean crystallizes, each increment is assumed to crystallize at the solidus (from [4]), where its temperature remains as the rest of the magma ocean crystallizes. Solid phases are calculated in equilibrium with the liquid, and their components subtracted from the remaining liquid. The liquid is crystallized from the bottom upward in shells of one half percent of the magma ocean. Solid phase compositions are not assumed to diffuse or reequilibrate, and no effects of interstitial liquids are included.

The phases crystallizing at each pressure are specified *a priori*: from 24-14 GPa, 50% majorite and 50% spinel crystallize. From 14-3 GPa, 10% garnet, 40% pyroxene, and 50% olivine crystallize, above which 40% pyroxene and 60% olivine crystallize. Equilibrium compositions for phases are calculated at each crystallization step by using exchange coefficients from the literature, and their densities are calculated for the pressure and temperature of solidification.

Results: *Crystallization models*: We present two models. The first, called the simple fractional crystallization model, is the result of fractionally crystallizing the magma ocean in the mineralogy described above. The second model, called the garnet segregation model, is a product of considering the density inversion at about 7.5 GPa. This inversion, the depth below which olivine and pyroxene float in their coexisting silicate liquid, has been discussed by previous researchers [5-8] and is reproduced by our calculations. However, previous models did not recognize that garnet sinks in this same pressure range. In our model garnet that crystallizes above 14 GPa sinks. As solidification proceeds, aluminum is exhausted from the remaining magma ocean liquid at about 11.4 GPa, and only olivine and pyroxene then fractionally crystallize from the remaining liquid.

The varying compositions of the crystallizing minerals lead to strong compositional stratification in the crystallized magma ocean. In both models, the deepest, majorite + spinel layer sequesters aluminum in the lowest layer of the mantle. Iron is increasingly enriched in the cumulates as crystallization proceeds, leading to the higher density of shallower cumulates. In the garnet segregation model, the garnet-rich layer is the densest and most aluminum-rich layer.

Overturn of the cumulates: The cumulate stratigraphy is gravitationally unstable in both models. Density distributions before and after overturn for the garnet segregation model are shown in figure 1. The resulting overturn may produce deep reservoirs segregated by density, bring cold material to the core-mantle boundary where it can cool the core, and carry hot material to shallower depths where it can melt adiabatically.

Overturn is idealized by sorting shells of the original stratigraphy so the density increases continuously with depth, resulting in a stable stratification. Each layer's composition and volume are conserved, and its temperature is adjusted for its adiabatic rise or fall. This overturn model assumes that freezing is fast compared to the overturn time of any solidified portion, and that cold downwellings from the top of the solidified layer completely displace deeper, lower-density layers, so that all layers are perfectly reshuffled.

During overturn, hot material rising from depth may cross its solidus, producing melt through depressurization. Because layers are reordered by density, the mid-mantle becomes a heterogeneous mix of deep and shallow material, leading to noncontinuous profiles in both composition and temperature. The overturn of the garnet segregation model produces a partially melted uppermost mantle to a depth of about 700 km (fig. 2). The temperature profile shown in figure 2 represents the energy available to produce melt, not the temperatures of the remaining solids after melting. When heats of fusion and incomplete melt segregation are taken into consideration, the melt is sufficient to create <100 km of crust over the planet s surface.

Later magmatism: The constraints on compositions and ages of reservoirs required by SNCs are consistent with a magma ocean crystallization scenario. Crystallization of the magma ocean produces a differentiated mantle, with enriched and depleted reservoirs. The constraint that the reservoirs are created by 10 - 100 Ma after accretion [9-12] is consistent with rapid magma ocean crystallization.

Following overturn, convection from thermal instabilities from the upper or lower boundary layers could melt the mid-mantle adiabatically and lead to long-term volcanism. The mid-mantle is depleted in Al_2O_3 and enriched in FeO in the garnet segregation model (fig.3). Melting of this material may be consistent with SNC major element compositions.

Early magnetic field: Overturn provides a possible mechanism for creating high core-mantle heat flow, and an attendant short-lived magnetic field. During overturn cold cumulates fall to the core-mantle boundary. Depending on the model, overturn creates a temperature difference across the core-mantle boundary of between 300 …C and 900 …C. Conductive heating of the lowermost mantle could sustain a heatflux out of the core for times on the order of a few hundred Myr. Convective instability of the lower mantle, if it has a sufficently low viscosity, could result in increased heat transfer over longer times, provided that compositional stratification preserves mantle reservoirs.

Conclusions: While the simple models presented here do not include all relevant physical processes, they are able to describe to first order the ages of differentiation and composition of mantle reservoirs, the moment of inertia factor of the planet, and they also provide a mechanism for magnetic field generation and cessation.

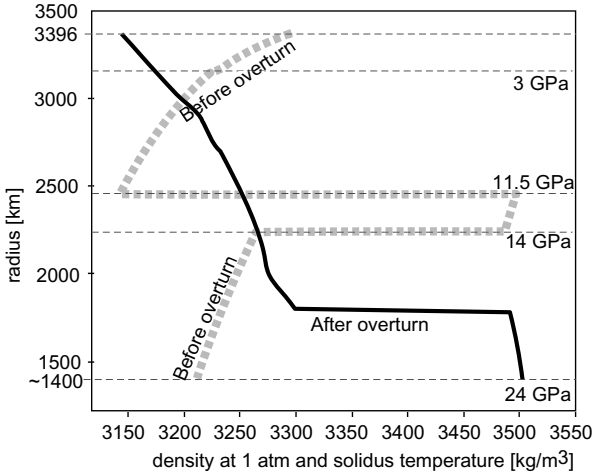

Fig 1: Density profiles before and after overturn for the garnet segregation model. During overturn, the dense, alumina-rich garnet layer falls to the core-mantle boundary.

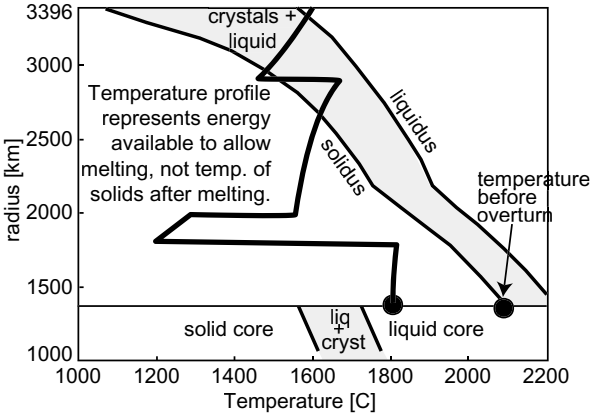

Fig 2: Solidus and liquidus for Martian compositions from [4]. Magma ocean crystallization begins at a potential temperature of approximately 2000 …C, and is complete at about 1100 …C. The temperature profile of the garnet segregation model after overturn is shown in the bold line.

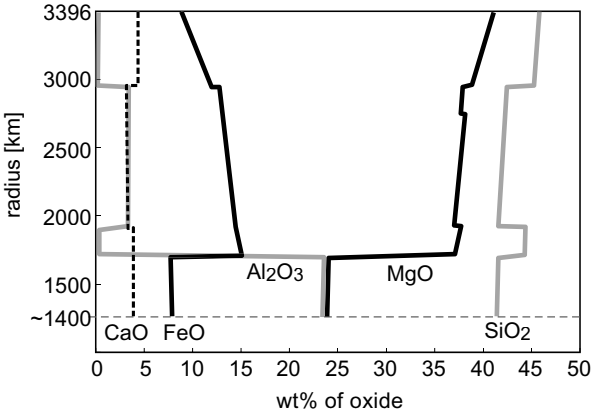

Fig 3: Compositional profiles after overturn for the garnet segregation model. The mid-mantle is enriched in FeO and depleted in Al_2O_3.

References: [1] Abe Y. (1997) *PEPI.* 100, 27-39. [2] Solomatov V.S. (2000) *In* R.M. Canup and K. Righter, eds. *Origin of the Earth and Moon*, U. AZ Press. [3] Bertka C.M. and Y. Fei (1997) *JGR.* 102, 5251-5264. [4] Longhi J., *et al*. (1992) in *Mars*, eds. H.H. Kieffer *et al*., U. AZ Press, 184-208. [5] Franck S. (1992) *PEPI*. 74, 23-28. [6] Morse S.A. (1993) *JGR*. 98, 5347-5353. [7] Stolper E.M. *et al.* (1981) *JGR*. 86, 6261-6271. [8] Agee C.B. and D. Walker (1988) *JGR*. 93, 3437-3449. [9] Shih C.-Y. *et al*. (1999) *Meteoritics* 34, 647-655. [10] Blichert-Toft J. *et al*. (1999) *EPSL.* 173, 25-39. [11] Borg L.E. *et al*. (2002) *GCA* 66, 2037-2053. [12] Herd C.D.K. *et al*. (2002) *GCA* 66, 2025-2036.